Ann. For. Res. 65(1): 11305-11322, 2022
ISSN: 18448135, 20652445

ANNALS OF FOREST RESEARCH
https://www.e-afr.org/

STUDY OF SAW-BASED HYDROGEN GAS SENSOR USING VARIOUS IDT MATERIALS AND GEOMETRY

Nimmala Harathi[1], Kavitha Subramanian[1]* and Argha Sarkar[2] and Rajakumar Selvarajan[3]

[1]Department of Electronics and Instrumentation Engineering, Annamalai University, 608002, Chidambaram, India.

[2]School of Computer science & Engineering, REVA University,562157, Bengaluru, India.

[3]Department of Manufacturing Engineering, Annamalai University, 608002, Chidambaram, India.

(*) Corresponding author:kaviraj_2003@rediffmail.com

Abstract

A 2D model of a SAW sensor is simulated using a variety of Inter Digitized Transducers (IDT) materials, with IDT heights varying from 100 to 150µm. Surface acoustic wave production depends critically on IDT. An additional amplification polymer layer is added to the SAW sensor's design to increase the sensor's sensitivity. Nanomaterials can enhance the device's functionality. To examine the sensor, Finite Element Modeling (FEM) is performed. The sensor's performance in relation to frequency is analyzed for deflection, electric potential, hydrogen gas, and noise. IDTs are made of copper, aluminum, and gold. Copper performs better than the other materials in terms of operating frequency at a minimum IDT height. The sensor's operating frequency is 355 MHz, and its displacement is 10 nm. With copper having the largest displacement and aluminum having the lowest displacement, the sensor's operating frequency remains constant for all materials. The sensor demonstrates a good agreement between the simulated operating frequency and the theoretical operating frequency. Hydrogen gas is also tested on the sensor at concentrations ranging from 1 ppm to 100 ppm. The sensor's reaction to the concentration of hydrogen has been linear. Calculations are made regarding the sensor's group velocity and phase delay. Group velocity and power spectral density are metrics that are used to express the phase noise of the sensor.

Keywords: SAW sensor, Deflection Analysis, Nanomaterials, Mass loading, White phase Noise, Flicker phase Noise.

1. INRODUCTION

SAW sensors became the centre of dynamic research in numerous fields but are not restricted to gas sensing, biomedical applications, automobiles, signal processing, and communications [1]. SAW sensors are passive devices since they do not require an external power source to function. Because of this nature SAW devices can be used in wireless applications in a harsh environment. The operating frequency of the saw devices varies from a few MHz to many GHz [2]. The SAW sensor mainly consists of a piezoelectric substrate, sensing layer, and two IDTs. The two IDTs are wrapped within a sensing layer and placed above the piezoelectric substrate. Out of two IDTs, one acts as an input IDT is called transmitter, and the second output IDT is called the receiver. At the transmitter IDT, electric signal gets converted to an acoustic signal and at the receiver, the acoustic

signal once again gets converted into an electric signal [3]. The acoustic signal is defined by its amplitude, frequency, and phase. The acoustic signal generated at the transmitter propagates over the sensing layer and experiences a change in its characteristics because of the sensing layer's electrical and Mechanical properties and the piezoelectric crystal properties. Deposition of analyte over the sensing layer allows for the analysis of the SAW sensor with a delay line structure that alters frequency. The analyte that is thusly deposited may be a biological agent, a gas, or a chemical solution. This study tests the SAW sensor for hydrogen gas. The presence of hydrogen gas results in a delay in the velocity of the SAW waves created on the surface, changing their frequency. The sensing layer's characteristics have an impact on the frequency shift as well. Numerous materials, such as composites, metals, semiconductor metal oxides, and polymers, can be deployed as sensing layers. Metal oxide semiconductors are the most often employed materials in the field of gas sensing because they have free electrons on their surface that interact with reducing or oxidative gas molecules. The design in the paper is concentrated with ZnO as sensing layer. This paper's design focuses on using ZnO as a sensor layer. One of the most promising materials in theField of sensors and optoelectronics is ZnO, an N-type II-IV, Wide and direct bandgap semiconductor with an approximate 3.37 eV and a substantial excitation binding energy (60 meV). Additionally, ZnO has a reasonably simple synthesismethod that enables structure control and produces oxygen vacancies, both of which have benefits for sensors that adsorb gas molecules. ZnO has also garnered interest for its affordability, simplicity of manufacture, excellent chemical stability, potential for doping, lack of toxicity, and ease of processing. ZnO guarantees a sizable specific surface area and permits gas molecules to enter the material's volume, which is very advantageous for SAW sensor detection. Another way to enhance ZnO sensor characteristics and get the best sensitivity is by creating heterostructures and functionalizing them with metals like Au, Pd, or P.

2.DESIGN OF THE PROPOSED SENSOR

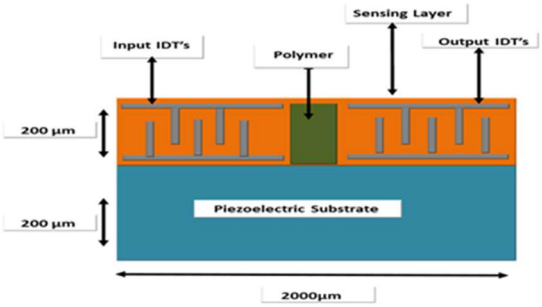

Figure 1.Front View of Proposed sensor.

The outline of the proposed sensor is shown in Figure 1. A two-dimensional SAW sensor is constructed with a lithium niobate (LiNbO3) piezoelectric substrate, sensing layer with ZnO and additional polymer layer Details of the proposed sensor's structure is given in Table 1.

Table1. Structural details of the proposed sensor

S.No	Name of the component	Dimensions

1.	Piezoelectric substrate	2000µm×200 µm
2.	Inter Digitated Transducers	2.5µm×140µm
3.	Sensing layer	2000µm×100µm
4.	Spacing between electrodes	2.5µm
5.	Pitch	100µm
6.	Anchor length	920 µm
7.	Anchor width	5 µm
8.	Anchor spacing	10 µm
9.	polymer width	100 µm
10.	polymer height	130 µm

Lithium niobate is chosen for its high electromechanical coupling coefficient given in Equation 1 to strengthen the SAW wave generated at the surface of the sensor with high bandwidth [4, 5].

$$K^2 = 2(V_f - V_m)/V_f \quad (1)$$

The electromechanical coupling coefficient K^2 is a function of metal phase velocityV_m, free surface phase velocity V_f.Ihe piezoelectric material constants used for simulation are shown in Table 2.

Table 2. Constants of piezoelectric material

S.No.	Name of the constant	Constant notation	Value
1.	Elastic constants [Pascal]	c11	2.02
		c12	0.573
		c13	0.752
		c14	0.085
		c33	2.424
		c44	0.595
2.	Piezoelectric constants [C/m3]	e15	3.69
		e22	2.5
		e31	0.3
		e33	1.77
3.	Permeability constants	ε11	45
		ε13	29
4.	Density[kg/m3]	ρ	47000

The arrangement of IDTs is shown in Figure 2. The anchor arrangement initiates the production of an acoustic wave due to the interaction between the electrostatic field of capacitance and the alternating electric field applied at the IDTs. Figure 3 shows the field distribution and acoustic wave generation at the IDT [6,7]. However, the net capacitance is the sum of individual Capacitance offered by the IDT pairs. IDT is the heart of the SAW sensor. The material used for IDT is one of the key factors affecting the sensitivity of the sensor. IDT can be constructed with a variety of materials like copper, silver, aluminum, platinum, and gold [8-10].

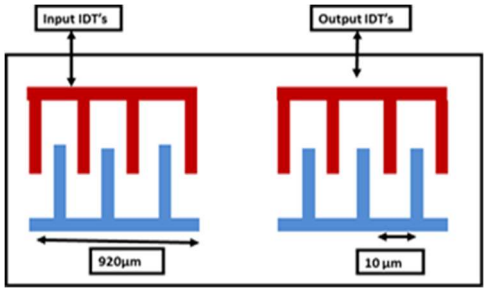

Figure 2. Structure of IDTs

The IDTs are provided with alternating potentials the electric field induced in the IDTs affects the electric field of the sensing layer. Hence, the deflection of the SAW sensor is a function of the physical and electrical properties of the IDT materials. The material constants of different IDT materials are given in Table 3.

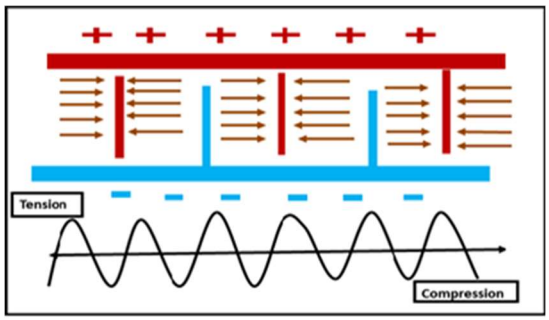

Figure 3. Field distribution at the IDTs

Table 3. Constants of various IDT & sensing layer materials

Parameter	Aluminum	Gold	Copper	ZnO
Density(Kg/m3)	2710	19300	8960	5610
Young's modulus(Gpa)	70	117	121	210
Poisson's Ratio	0.35	0.34	0.34	0.358
Shear Modulus (Gpa)	26	48	44	68
Bulk Modulus (Gpa)	76	140	154	144

3.MATHEMATICAL MODELING OF PROPOSED SENSOR

The significant parameters governing the SAW sensor is operating frequency, surface electric potential and total capacitances of IDT. The operating frequency of the SAW sensor is a function of acoustic velocity V and operating wavelength λ expressed in Equation 2.

$$F = V/\lambda \qquad (2)$$

The acoustic velocity of the SAW sensor depends on the young modulus ε and ρ density of the piezoelectric substrate expressed in Equation 3.

$$V = \sqrt{\varepsilon / \rho} \quad (3)$$

$$\lambda = 2(W_e + W_{sp}) \quad (4)$$

The wavelength is also expressed in terms of the geometry of the SAW sensor i.e. width of IDT W_eand spacing between IDTs W_sp expressed in Equation 4. In this construction the spacing between IDTs is considered 5 µm, the width of the electrode is 5µm with λ as 20 µm.

$$d = eS + \varepsilon E \quad (5)$$

$$T = cS - eE \quad (6)$$

The generated acoustic wave propagates over the sensing layer with a deflection expressed in terms of stress given in Equation 5 and electric displacement given in Equation 6. The stress (T) developed on the surface of the sensor with electric displacement (d) is a function of dielectric, strain matrix, dielectric and piezoelectric matrix (ε) [11]. Equation 7 shows the total capacitances of IDTs as a function of operating frequency $f0$ and impedance of IDT pair Z. The bandwidth of the sensor is the function of the number of IDTs wrapped within the sensing layer. The sensor is constructed with 92 pairs of IDTs on either side of the sensing layer.

$$C_t = \frac{1}{2\Pi f_0 Z} \quad (7)$$

The functional relationship between operating frequency and the number of IDT pairs is given in Equation 7. Ct is the total capacitance of the IDT. f_0 is the operating frequency of the sensor. Z is the impedance of the IDT pair. The arrangement of IDTs resembles parallel plate capacitors supported with two anchors on the top and bottom [12,13]. Gas sensing is one of the most significant uses for SAW sensors. The mass of sensing layer changes due to the selective molecule adsorption. It is caused by the external gas, chemical mixture, and foreign particles that are deposited over it. Expression 8 shows that the frequency shift of the sensor is a function of the mass of the sensing layer and acoustic velocity, the mass-loading effect of the sensing layer causes a change in frequency.

$$\Delta f = K f_0^2 \frac{M}{A} \quad (8)$$

M is the mass of the sensing layer, A is the area of the sensing layer, and F_0 is the center frequency. K is the material's coefficient of mass sensitivity.

$$\frac{\Delta F}{F_0} = \frac{\Delta M}{M} = \frac{\Delta V}{V} \quad (9)$$

According to expression 9, the sensing layer's mass and acoustic velocity affect the sensor's frequency shift. Here, F is the frequency shift, F_(0)is the center frequency, V is the change in acoustic velocity.

4. RESULTS AND DISCUSSION

The presented two-dimensional sensor is constructed in comsol multiphysics using electrostatics and piezoelectric studies. The electrostatics is used to set the boundary lines for the sensor with longitudinal periodic limits and zero potential at the surface and base of the sensor. Electrostatics is used to apply alternating floating and zero potentials to the IDT pairs [14-16]. Piezoelectric studies help in defining coupling coefficients, elastic coefficients, dielectric constants, and piezoelectric coefficients causing electric and piezoelectric charge conversion over the piezoelectric substrate and sensing layer. A specific list of materials is contained in the Comsol software's material database. The database contains the materials used to build the sensor layer and the piezoelectric substrate. Since polymer is not included in the Comsol material list, it can be added by including the necessary parameters, such as young's modulus, poisons ratio, and relative permittivity. The additional material may be deposited on the structure. The 2D designed sensor is shown in Figure 4. The sensor is meshed with fine mesh particles shown in Figure 5. Figure 6 depicts the formation and spread of SAW waves over the sensor's surface. The SAW wave is quite distinct, with alternating tough peaks and crests over the surface. The highest peaks in the sensing layer correspond to the region's maximum deflection.

4.1. Analysis of sensor

The behavior of the sensor is investigated for deflection analysis with frequency, the effect of IDT height on the deflection, and deflection analysis for different IDT materials [17-20].

4.1.1 Deflection Analysis

In this study, performance of the sensor is examined for aluminum, copper, and gold. Figure 7 shows the displacement response of three materials at 100μm. The density of IDT is one of the key parameters affecting the deflection of the sensor. Among these three materials, aluminum has low density and gold has high density. A fractional change in the density of IDT causes a change in the mass density of the sensing layer which in turn affects the electric field produced over the surface of the SAW sensor. From Equation 5 it is evident that deflection of the sensor is a function of the electric field produced over the surface of the sensor.

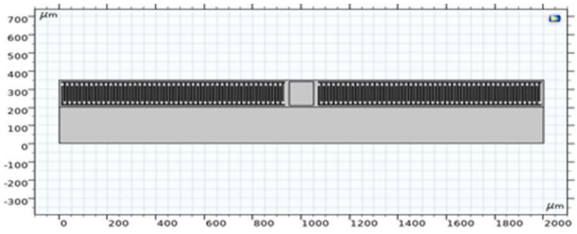

Figure 4. Proposed sensor construction.

In addition to the physical parameters, electrical parameters like electrical conductivity also influence the deflection of the sensor. Out of three materials, copper has the highest electrical conductivity and aluminum has the lowest electrical conductivity.

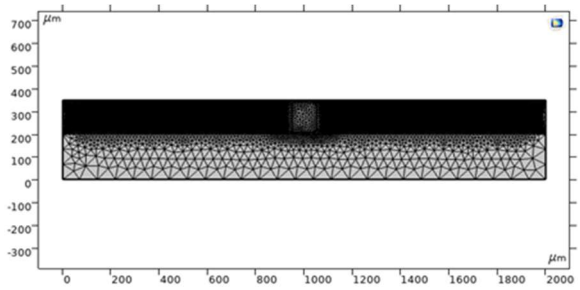

Figure 5. Meshing of sensor.

In the present simulation work, the operating frequency of the sensor is 355 MHz with the highest displacement for all the three IDT materials. This operating frequency is in close approximation to the theoretical calculations.

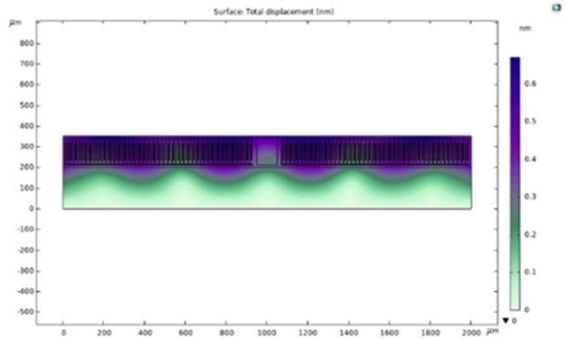

Figure 6. SAW wave propagating on the surface of the sensor.

The sensor has a second deflection peak at 378 MH4z with a magnitude less than that of the first peak. Among the three materials copper has shown the highest deflection at 100μm of IDT height with a peak deflection of 9.98nm. Poor density and young's modulus of the aluminum signifies the low deflection at the operating frequency. As though the density of gold is very high compared to copper and aluminum its deflection peaks are moderate at two frequencies because of its moderate electrical conductivity and moderate young's modulus among three materials.

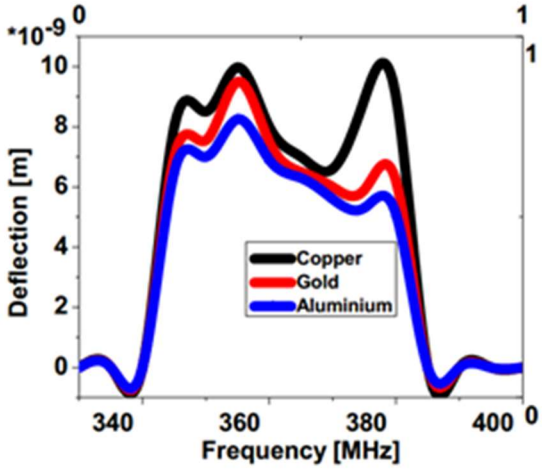

Figure 7. Deflection Analysis of proposed sensor.

4.1.2 Analysis of Electric Potential

Figure 3 clearly shows the electric field distribution in the sensing layer. The sensing layer withholds the IDTs and a polymer layer for amplification of deflection. The electric potential developed over the surface of the SAW sensor is a function of the electrical properties of constituents of the sensing layer. The electric potential amplification in the sensing layer for the proposed sensor is clearly shown in Figure 8. The alternating floating and ground potentials offered at the input and output IDTs are justified by the potential distribution. Figure 9 shows the electric potential distribution of the sensor. ZnO is one of the best available metal-oxide-based semiconductors with bio-compatible properties. ZnO is highly influenced by its doping materials. ZnO with piezoelectric material doping behaves as an insulator and with n-type doping material becomes a pure conductor. With the characteristics of an insulator and conductor ZnO is said to be a metal-based semiconductor with dual compatible properties.

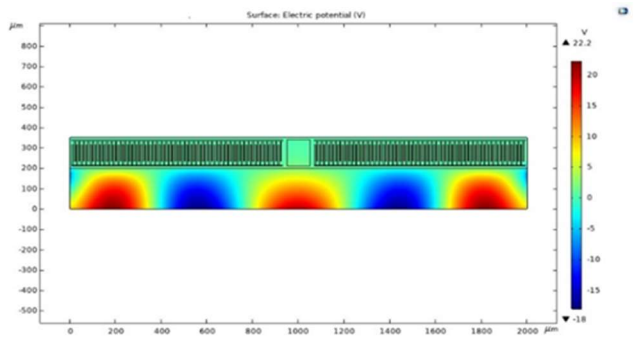

Figure 8. Electric potential distribution of proposed sensor.

The three IDT materials are trivalent acceptor P-type impurities. The recombination between acceptor impurities and ZnO results in the formation of n-type material leading to a change in electric conductivity over the surface of the SAW sensor. The increasing order of electric conductivity of three IDT materials is aluminum, gold, and copper.

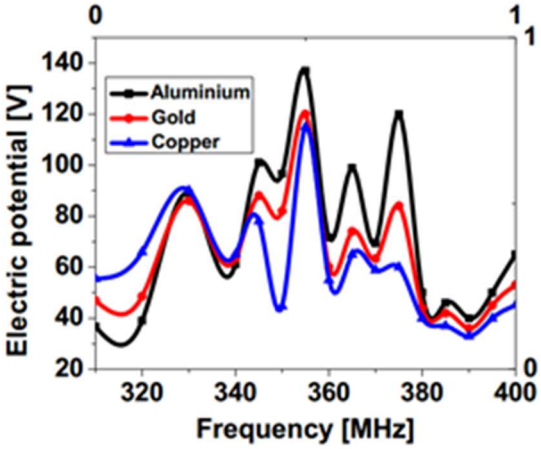

Figure 9. Electric potential distribution of proposed sensor.

Higher conductivity is due to low resistance causing low electric potential. Aluminum has the highest electric potential to low electrical conductivity and copper has low electric potential with high electric conductivity and vice-versa.

4.2Study of IDT Material as a function IDT Geometry

IDT geometry is also one of the foremost specifications influencing the performance of the SAW sensor. The IDT is geometry is governed by width, height, and spacing between IDTs. This study also focused on the IDT geometry by increasing the height in steps of 10µm from 100µm to 150µm.

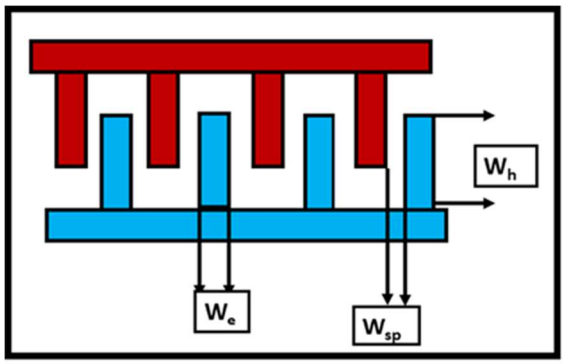

Figure 10. Structure of single pair IDT.

Figure 10 shows the structure of single pair IDT with anchors. From equation (3) it is very clear that the wavelength of the acoustic wave is a function of the width of the electrode and the spacing between the electrodes. The height of the electrode is an integral multiple of the wavelength of acoustic waves like 5λ, 10λ, 15λ, 20λ,… etc. With the increase in the height of the IDT, the strain over the surface of the sensor increases affecting the electrical conductivity [24-26], with the decrease in the electrical conductivity the deflection of the sensor decreases. The maximum deflection of the sensor is obtained at the minimum IDT height for all three materials.

4.2.1 Deflection of Aluminum

Aluminum occupies 8.1 percent of the earth's crust. Being the 13th element in the periodic table it is light in weight and durable in functionality. It is a donor impurity that donates an electron. On other side of the sensing layer, zinc oxide is a semiconductor group with a band gap of 3.37eV.

Figure 11 shows the deflection analysis of aluminum for different IDT heights [27-28]. The deflection is studied with varying IDTs height from 100µm to 150µm in steps of 10µm. The pattern of deflection at all heights is consistent, however the magnitude decreases as IDT height increases. This inverse relationship results from the SAW wave's magnitude decreasing as IDT height increases. The interaction between aluminum and ZnO leads to displacement reaction causing a change in electrical conductivity Aluminum IDTs with increasing heights in reaction with zinc oxide in the sensing layer to affect the deflection in reducing factor.

These IDTs obtained maximum deflection in order of 8nm with an operating frequency of 355 MHz The second response peak is very less at 378MHz because of the displacement reaction

effect. The response of the sensor at all the IDTS heights is similar with zero deflection at minimum and maximum frequencies. The response is quite good in the mid-band frequencies from 300 MHz to 400 MHz.

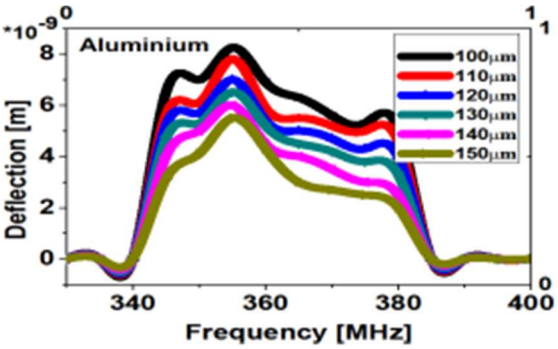

Figure 11. Performance of aluminum with varying IDT height.

4.2.2 Deflection of Gold

Gold is one of the precious metals belonging to the donor impurity with high thermal and electrical conductivity. ZnO can be doped to various metals leading to different reactions like oxidation and reduction action. The interaction between ZnO and gold leads redox reaction. Figure 12 shows the performance of gold IDT With the increasing heights from 100μm to 150 μm with increment of 10μm. Among the three materials used for IDT construction, the gold has moderate density and young's modulus indicated the change in the electric

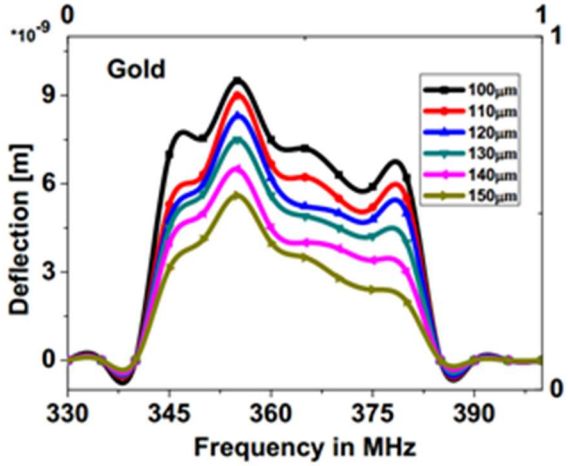

Figure 12. Performance of gold with varying IDT height.

conductivity is moderate with the changes in physical parameters The stress that is created by hydrogen gas deposition over the sensing layer causes an acceptable change in electric conductivity, which in turn influences the deflection on the sensor's surface. As IDT height rises, the crest and tough of the SAW wave are suppressed, which lowers the peak of deflection. The deflection of the sensor is in order of 9nm at the operating frequency and the second peak is in

order of 7nm with the frequency of 378Mhz. Gold shows an average deflection at the second peak because of its physical and chemical behavior.

4.2.3 Deflection of Copper

Like silver and gold, copper belongs to the same group in the periodic table. Copper is colorless being a part of donor impurity as that of other IDT materials. Copper has high thermal and low resistivity leading to better electric conductivity. Figure 13 shows the response of copper IDT with varying heights of IDT. Copper has a high young's modulus along with high bulk and shear modulus with moderate density compared to the other two metals. ZnO on other hand is a reducing agent that interacts with copper leading to a redox reaction. The redox results in a drastic change in electrical conductivity over the surface of the sensor. The IDT geometry,material and sensor layer characteristics determine the SAW wave's magnitude.The SAW wave's crest and tough are reduced as IDT height increases, bringing down the peak of deflection The peak of deflection of copper is in terms 10nm with operating frequency of 355MHz. Copper shows variant behavior than aluminum and gold because of its high conducting nature. The second peak of copper has a close approximation to the first peak.

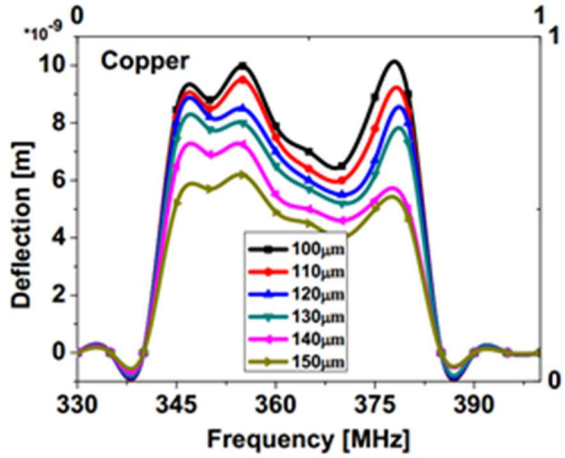

Figure 13. Performance of copper with varying IDT height.

4.3 Performance of Different Materials

Figure 11, 12 and 13 show the deflection of different IDT materials with varying heights of IDT. Three different materials are used for construction; gold shows the linear deflection with the height of IDT. This linearity is because of the electrical (conductivity) and physical (density, bulk, and shear modulus) parameters of gold. Aluminum and copper have a slight deviating nature at the mid-height of IDT due to fluctuating physical and thermoelectric proprieties.

4.4 Response of the Sensor to Hydrogen Gas

Hydrogen gas is combination of two H molecules with covalent bonding between them. Hydrogen is odorless gas and color less gas with affinity towards oxygen. Hydrogen is released as a result of the thermochemical reaction and fuel combustion. When hydrogen levels are exceeded, respiratory issues can become fatally extended for long periods of time. Therefore, it is crucial to

detect hydrogen gas. The sensing layer is constructed with ZnO which is a semiconductor material, whose characteristics changes with external gas. Deposition of hydrogen gas over the sensing layer causes leads to change in the mass of the sensing layer. Figure 14 shows the concentration of gas verses deflection of the sensor.

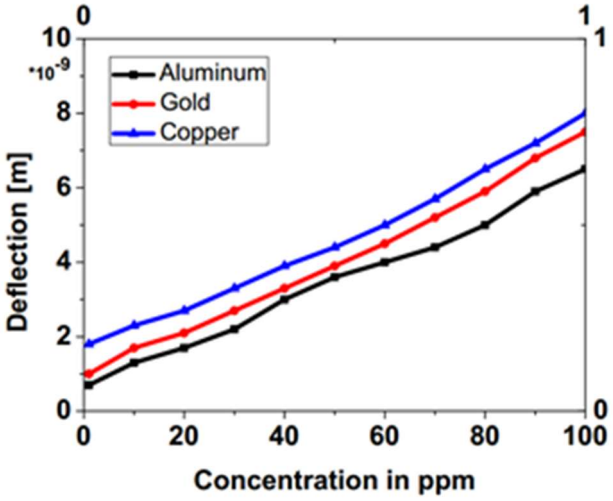

Figure 14. Deflection Analysis of the sensor with hydrogen gas.

The mass of the sensing layer is affected by changes in gas concentration across the sensor's surface, which has an impact on how much the SAW wave deflects over the sensor's surface. The SAW sensor's deflection decreases as the sensing layer's mass grows due to increased surface tension. Expression 9 clearly states the relationship between changes in mass with respect to frequency. Figure 15 shows the variation of frequency with respect to concentration of hydrogen gas.

The mass loading over the surface of the sensing layer and the gas concentration have a linear relationship, which results in a linear relationship with the change in frequency.

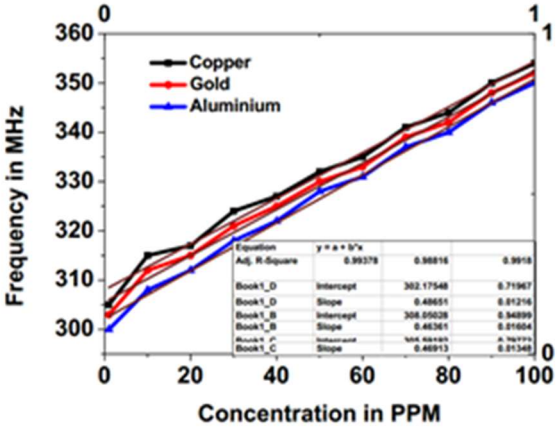

Figure 15. Frequency Analysis of the sensor with hydrogen.

Figure 16 shows the variation of frequency shift with the concentration of the gas. Due to the linear relationship between the mass loading effect and frequency shift, the relationship between frequency shift and gas concentration is linear. Among the three materials, copper has low-frequency shift and aluminum has the highest frequency for hydrogen gas. Despite having a low

density compared to the other two IDT materials, copper's high young's modulus reduces the impact of mass loading.

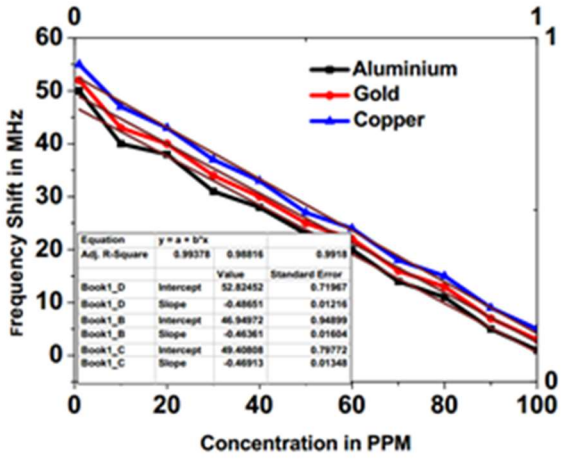

Figure 16. Frequency analysis of the sensor with hydrogen gas.

4.4 Noise Analysis of the Sensor

Noise is defined as random variations in the sensor output brought on by unrelated variations in the input. Noise in SAW sensor is due to the additive fields developed by the IDT's, mass loading effect and electric potential of the sensing layer [30-34]. The electric field produced by the IDT's, which varies with the material of the IDT and the mass effects of gas, causes delay in the phase and velocity of the SAW signal.

Table 4. Summary of sensor operating parameters

Specification	Value
Length of the delay line	L=100µm
Acoustic wavelength	λ=10
Center Frequency	Fo=344.8MHz
Frequency shift	Δf=6.55 MHz
Phase velocity	Vψ= Fo λ=3488m/s
Phase delay	Tψ=L/ Vψ=28.66ns
Phase slope of delay line	Δψ/Δf=-13.5 rad/MHz
Group Delay	Tg= Δψ/(Δf 2Π)=2.126 sec
Group velocity	Vg=L/ Tg=47 µm/s
Electrical sensitivity	2Π Tg=13.35 rad/MHz

This results in phase delay of the signal causing random fluctuations on the surface of the SAW sensor. Hence the noise signal of SAW sensor is function frequency of the sensor. The different noises experienced by the SAW sensor are white phase noise and flicker phase noise. The SAW wave's phase changes as a result of the frequency of the sensor, which causes flicker phase noise. White phase noise is produced by amplification stages of flicker phase noise. History shows that

the SAW sensor's noise is represented by the power spectral density of phase fluctuations S_Ψ (f) with always n≤4.The noise function of SAW sensor is given in Equation 10. Table 4 shows the sensor functional parameters with its specific values. The S_Ψ (f) denotes the noise function, b is the magnifying parameter of SAW sensor and F is operating frequency of the sensor.

$$S_{\varphi}(f) = \Sigma_{i=-n}^{0} b_i f^i \qquad (10)$$

For n=0 and n=-1 denotes white phase noise and1/f represents flicker phase noise. Figure 17 shows the power spectral density of phase fluctuations as a function of frequency. The power spectral density is expressed in terms of dB rad2/Hz.

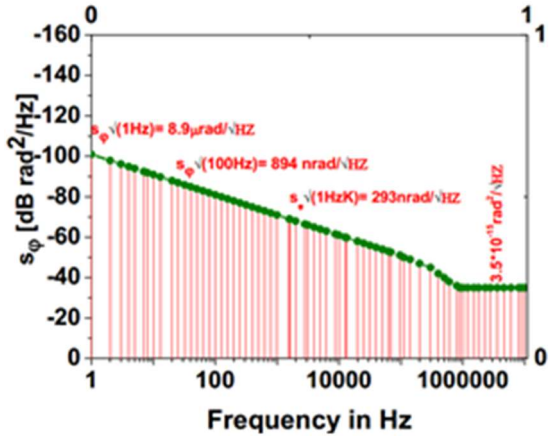

Figure 17. Power spectral density of phase noise

At higher frequency the spectral power density is almost stable. Phase noise can be eliminated using phase noise suppression function shown in Figure 18. The phase noise suppression function is shown in Equation 11. It is a function of operating frequency f and group delay T_g.

$$PNS(f, \tau_g) = 20\log_{10}(2\sin(\pi f \tau_g)) \qquad (11)$$

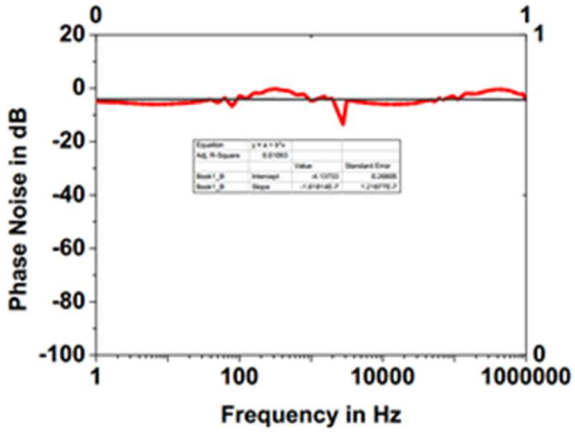

Figure 18. Power Spectral Density of Phase Noise

Phase delay and phase velocity has to be minimized to minimize phase noise. The Noise of the proposed sensor is in and around -6dB to -13dB. The phase noise is almost remains constant at low frequency and till fluctuating in the mid frequency and stable at high frequency as the sensor goes saturated.

5. CONCLUSION

A two-dimensional SAW sensor with an amplification layer is designed using Comsol multiphysics. The behavior of the sensor is studied for various IDT materials like aluminum, gold, and copper with varying heights of IDT from 100μm to 150μm. The response of the sensor is studied for deflection, operating frequency, deflection for varying IDT material, and deflection for varying IDT height. The operating frequency of the sensor is the same for all the materials and all heights of IDTs as the width of the IDT and spacing between the IDT remain the same. The operating frequency of the designed sensor is 355MHz with maximum deflection. The three materials used for IDT are donor impurities belonging to the same group in the classification of metals. All the three materials interact with the dual behavior ZnO sensing layer leading to reducing and oxidation reactions causing a change in electrical conductivity at the surface of the sensor. From the material behavior it is very clear that copper has high conductivity and aluminum with low levels. For the proposed sensor copper IDT has shown the highest deflection at the operating frequency. All the three materials obtained a second response peak at 378MHz with a deflection less than that of the first peak. The sensor is also studied for varying heights of IDT. The response of the sensor is good at minimum IDT height rather than higher heights of IDT. With the increase in the height of IDT, the stress over the surface of the sensor increases decreasing the electric conductivity on the surface of the sensor. With three different IDT materials and varying IDT heights, the response of copper IDT at minimum IDT height is good compared to the other responses of the sensor. From the response, it is clear that the deflection is in increasing order of aluminum, gold, and copper. The response of the sensor to hydrogen gas is proportional to its concentration. In the presence of hydrogen gas, copper has demonstrated a low frequency shift from the working frequency. Despite having a moderate density, copper has a high enough Young's modulus to lessen the impact of mass loading on the sensor's surface.

The noise fluctuations in the sensor are analyzed and recorded. The mass loading effect on the sensor's surface, the phase, velocity delay caused by IDT's field dispersion accounts for the sensor's noise. SAW sensors are prone to white phase noise and flicker phase noise. The phase noise in the sensor is expressed as power spectral density function expressed in terms of dB rad2 /Hz. The power spectral density plot clearly shows that the phase noise remains constant with a value of 3.5x10-15 rad2/Hz at high frequency. Phase noise suppression is the key factor to suppress the phase noise. The phase noise suppression is function of group phase delay. By minimizing the phase delay and velocity delay phase noise can be suppressed.

ACKNOWLEDGEMENT

The authors would like to acknowledge Annamalai University for providing the Comsol Multiphysics software and infrastructure support.

CONFLICT OF INTEREST

The authors declare that they have no known contest for financial interests or personal engagements that could have appeared to influence the work reported in this paper.

REFERENCES

- Priya, R., Banu, T., Venkatesan, G., Pandiyarajan., Haresh M. Pandya., "A short review of saw sensors", J. Environ. Nanotechnol, 4 (2015) 15-22.
- Karapetyan, G.Y., Kaydashev, V.E., Kutepov, M.E., Minasyan, T.A., Kalinin, V.A., Kislitsyn, V.O. and Kaidashev, E.M.,"Passive wireless UV SAW sensor" , Appl. Phys, 126 (2020) 1-9.
- Gálik, G., Kutiš, V., Murín, J., & Lalinský, T., "3D FEM model of piezoelectric SAW sensor", Proc. 20th Inter. Conf. on Applied Phys. of Cond. Matter (APCOM 2014), (2014) 316-319.
- Luo, W., Fu, Q., Deng, J., Yan, G., Zhou, D., Gong, S.,Hu, Y., "An integrated passive impedance-loaded SAW sensor", Sens. Actuators B Chem, 187 (2013) 215-220.
- Sarkar, A., Venkataramana, P., Harathi, N., Jyothsna, T., Teja, N. V., "Design and optimization of ZnO nanostructured SAW-based ethylene gas sensor with modified electrode orientation", Adv. Sci. Technol. Eng. Syst, 5 (2020) 263-266.
- Valluru, S. P. R.,"Design of FIDT for 3D analysis of MEMS based gas sensor using SAW technology", Proceed. Comsol Conf, (2015).
- Harathi, N., Kavitha, S., Sarkar, A., "ZnO nanostructured 2D layered SAW based hydrogen gas sensor with enhanced sensitivity", Materials Today: Proceedings, 33 (2020) 2621-2625.
- Harathi, N., Sarkar, A., "TiO2 based surface acoustic wave gas sensor with modified electrode dimensions for enhanced H2 sensing application", Int J Nano Dimens, 12 (2021) 83-89.
- Kavitha, S., Daniel, R. J., Sumangala, K., Kavitha, S., "High performance MEMS accelerometers for concrete SHM applications and comparison with COTS accelerometers", Mech. Syst. Signal Process, 66 (2016) 410-424.
- Mohanan, A. A., Islam, M. S., Ali, S. H. M., Parthiban, R., Ramakrishnan, N., "Investigation into mass loading sensitivity of sezawa wave mode-based surface acoustic wave sensors", J. Sens,13 (2013) 2164-2175.
- Li, H., Liu, X., Li, L., Mu, X., Genov, R., Mason, A. J., "CMOS electrochemical instrumentation for biosensor microsystems: A review", J. Sens, 17 (2016) 74.
- Devkota, J., Kim, K. J., Ohodnicki, P. R., Culp, J. T., Greve, D. W., Lekse, J. W., "Zeolitic imidazolate framework-coated acoustic sensors for room temperature detection of carbon dioxide and methane", Nanoscale, 10 (2018) 8075-8087.
- Zhang, G., "Nanostructure-enhanced surface acoustic waves biosensor and its computational modeling", J. Sensors, (2009).

- Han, J., Li, M., Li, H., Li, H., Li, C., Li, H., Yang, B., "A 433-MHz surface acoustic wave sensor with Ni-TiO2-poly (L-lysine) composite film for dopamine determination", Microchimica Acta,187 (2020) 1-10.
- Scholl, G., Schmidt, F., Ostertag, T., Reindl, L., Scherr, H., Wolff, U., "Wireless passive SAW sensor systems for industrial and domestic applications", In Proceedings of the 1998 IEEE International Frequency Control Symposium (Cat. No. 98CH36165), (1998) 595-601.
- Qiao, D., Liu, W., & Smith, P. M., "General Green's functions for SAW device analysis", IEEE transactions on ultrasonics, ferroelectrics, and frequency control, 46 (1999) 1242-1253.
- Luo, W., Fu, Q., Deng, J., Yan, G., Zhou, D., Gong, S., Hu, Y., "An integrated passive impedance-loaded SAW sensor", Sens. Actuators B Chem., 187 (2013) 215-220.
- Khan, S., Lehana, P., Arya, S. "Fabrication and characterization of focused interdigital transducer based Pd/ZnO/n-Si SAW sensor", Sensor Letters, 15 (2017) 219-226.
- Hoang, T., Beghi, M. G. "SAW parameters analysis and equivalent circuit of SAW device", Acoustic Waves-From Microdevices to Helioseismology, (2011) 443-482.
- Cai, H. L., Yang, Y., Zhang, Y. H., Zhou, C. J., Guo, C. R., Liu, J., Ren, T. L., "A high sensitivity wireless mass-loading surface acoustic wave DNA biosensor", Mod. Phys. Lett. B, 28 (2014) 1450056.
- Ieki, H., Kadota, M., . "ZnO thin films for high frequency SAW devices", In 1999 IEEE Ultrasonics Symposium. Proceedings. International Symposium (Cat. No. 99CH37027), 1(1999) 281-289.
- Zakaria, M. R., Hashim, U., Amin, M. M., "Design and fabrication of IDT saw by using conventional lithography technique", Middle East J. Sci. Res, 18 (2013) 1281-1285.
- Tang, G., Han, T., Teshigahara, A., Iwaki, T., Hashimoto, K. Y., "Enhancement of effective electromechanical coupling factor by mass loading in layered surface acoustic wave device structures", Jpn. J. Appl. Phys, 55 (2016) 07KD07.
- Emanetoglu, N. W., Gorla, C., Liu, Y., Liang, S., Lu, "Epitaxial ZnO piezoelectric thin films for saw filters", Mater Sci Semicond Process MAT SCI SEMICON PROC, 2 (1999) 247-252.
- Kutiš, V., Gálik, G., Královič, V., Rýger, I., Mojto, E., Lalinský, T., "Modelling and simulation of SAW sensor using FEM", Procedia Eng, 48 (2012) 332-337.
- Scholl, G., Schmidt, F., Ostertag, T., Reindl, L., Scherr, H., Wolff, U., "Wireless passive SAW sensor systems for industrial and domestic applications", Proceedings of the 1998 IEEE International Frequency Control Symposium (Cat. No. 98CH36165), (1998) 595-601.
- Ahmadi, S., Hassani, F., Korman, C., Rahaman, M., Zaghloul, M., "Characterization of multi- and single-layer structure SAW sensor [gas sensor]", Sensors, (2004) 1129-1132.
- Sato, M., Yamamoto, T., Meguro, T., Yamanouchi, K.,"Sensitivity of an anodically oxidized aluminium film on a surface acoustic wave sensor to humidity", Sens. Actuators B Chem, 20 (1994) 205-212.
- Harathi, N., Bollu, M., Pasupuleti, K. S., Tauanov, Z., Peta, K. R., Kim, M. D., Rao, V. N., "PrGO decorated TiO2 nanoplates hybrid nanocomposite for augmented NO2 gas detection

with faster gas kinetics under UV light irradiation", Sens. Actuators B Chem, 358 (2022) 131503.

- Durdaut, P., Kittmann, A., Rubiola, E., Friedt, J. M., Quandt, E., Knöchel, R., Höft, M., "Noise Analysis of Open-Loop and Closed-Loop SAW Magnetic Field Sensor Systems", arXiv preprint arXiv, (2019) 1901.01428.
- Mauder, A., "SAW gas sensors: comparison between delay line and two port resonator", Sens. Actuators B Chem, 26 (1995) 187-190.
- Kavitha, S., Daniel, R. J., Sumangala, "Design and analysis of MEMS comb drive capacitive accelerometer for SHM and seismic applications", Meas. Tech, 93 (2016) 327-339.
- Chen, X., Cao, M., Li, Y., Hu, W., Wang, P., Ying, K., & Pan, H., "study of an electronic nose for detection of lung cancer based on a virtual SAW gas sensors array and imaging recognition method" ,Meas. Sci. Technol, 16 (2005) 1535.
- Harathi, N., Subramanian, K., Sarkar, A., Selvarajan, R., "Performance Evaluation of SAW-Based Hydrogen Gas Sensors with Different IDT Geometries", Nano LIFE, 12 (2022) 2250009.